JOURNAL OF CATALYSIS 9, 76–86 (1967)

The Effect of Foreign Ions on the Stability of Activated Alumina

R. M. LEVY AND D. J. BAUER

From the Central Research Department, Monsanto Company, St. Louis, Missouri 63166

Received July 5, 1967

The thermal stability and physical properties of a spinel-structure, activated alumina are studied as a function of the precursor material, a low-temperature, highly amorphous alumina impregnated with varying concentrations of Li^+, K^+, or Mg^{2+}. Measurements of physical properties such as surface area, density, and pore volume, and spectroscopic data from X-ray diffraction and the Mössbauer effect are allied in the characterization of the bulk and surface occupation of the foreign ions and the effects of these on thermal stability. Foreign-ion contents leading to maximum stability are determined.

INTRODUCTION

Despite the great applicability of high-surface-area alumina as a common support in heterogeneous catalysis, and a substantial body of data relating the physical and chemical variables, a complete understanding of the surface and bulk properties of this material does not yet exist. Spectroscopic (*1*), electrical (*2*), crystallinity (*2*), and chemical (*3*) information do describe, to some extent, the intrinsic structure of activated aluminas, but prediction and control of physical and chemical properties are as yet quite tentative.

This paper reports a study of the effects of doping agents upon the physical properties of a commercially available, high-surface-area alumina. The data suggest a mechanistic and systematic approach for the optimization of physical stability of an activated alumina through proper concentration of doping agents, and give a plausible basis for the stabilization previously alluded to in the patent literature (*4*).

METHODS

Materials. The starting alumina in these studies was Kaiser KA-101-10 [(-10) designates the specific lot of KA-101 studied]. This was initially received as a primarily amorphous, low-temperature modification with an X-ray pattern approaching that of gamma alumina and physical properties similar to eta alumina (*2*). The material was prepared, according to the producer, by dehydration of gibbsite followed by an activating rehydration and dehydration cycle on the resultant poorly crystalline pseudoboehmite intermediate. The alumina, as received, had a surface area of 278 m^2/g and a total pore volume of 0.55 cm^3/g. Impregnates of reagent-grade nitrate salts of lithium, potassium, and magnesium were incorporated using an aqueous solution with a volume just sufficient to be completely absorbed by the dry alumina. Concentrations were continuously varied between 0 and 0.06 impurity-to-aluminum ion ratio.

Calcination. Heat treatments of all samples were carried out under controlled atmosphere in a Lindbergh Hevi-duty tubular oven. Two atmospheric conditions were used: dry air at a flow rate of 800 cm^3/min, and a 3:1 air-to-steam mixture also at a total gas flow of 800 cm^3/min. Gases were preheated before admission to the sample tube.

Alumina charges of 100 cm³ were packed in a 55-mm-diameter quartz tube between insulating layers of Vycor Raschig rings. Samples were heated to 450°, 600°, 700°, 800°, 900°, and 1000°C. Temperatures were rapidly brought to within 100° of the final value and a variable-current automatic controller then set at the predetermined reading for the desired temperature. At this time, an automatic timer, set for 5 hr, was activated. Resultant temperatures, measured by a thermocouple probe contained in a quartz thermowell, varied by less than 15° from the desired value over the length of the alumina bed. Samples were allowed to cool slowly under a stream of dry nitrogen.

Physical measurements. Surface-area determinations were carried out by the standard BET technique (*5*). Duplicate runs assured an error of less than 5%. Macropore volumes (pores with openings greater than 700 Å in diameter) and particle density (Hg displacement under atmospheric pressure) were measured on an Aminco mercury porosimeter, the macropore volumes being those measured by application of a mercury pressure of 2500 psi. True density, or helium displacement, was determined on a Beckman air pycnometer adapted for use with helium atmospheres, and total pore volume was calculated from the particle density and true density data.

Spectroscopic measurements will be described in the pertinent sections.

Results

Physical Properties

A large volume of work has previously been published concerning the kinetics and mechanism of thermal loss of surface area of alumina, as measured by time-dependent values of parameters such as pore volume or density. Workers at Shell Development Co. assigned this loss of the surface area, or sintering, to diffusion of ions on or near the surface and formation of fillets of material connecting adjacent particles (*6, 7*). This mechanism is substantiated by an electron-microscope verification of the growth of large particles during the sintering process (*8*), and is readily characterized by a change in distribution of pore diameters.

The data presented here represent a study of the effect on the rate and nature of thermal equilibration of the surface, of starting materials: foreign ions impregnated on a specific alumina. Although measurements were performed upon samples

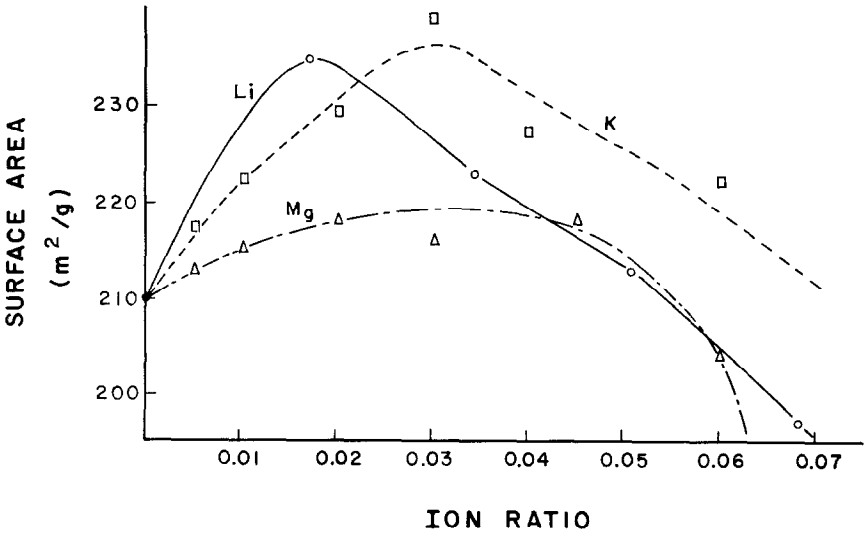

FIG. 1. Surface areas of impregnated aluminas heated in dry air for 5 hr at 600°C. Probable errors are ±10 m²/g.

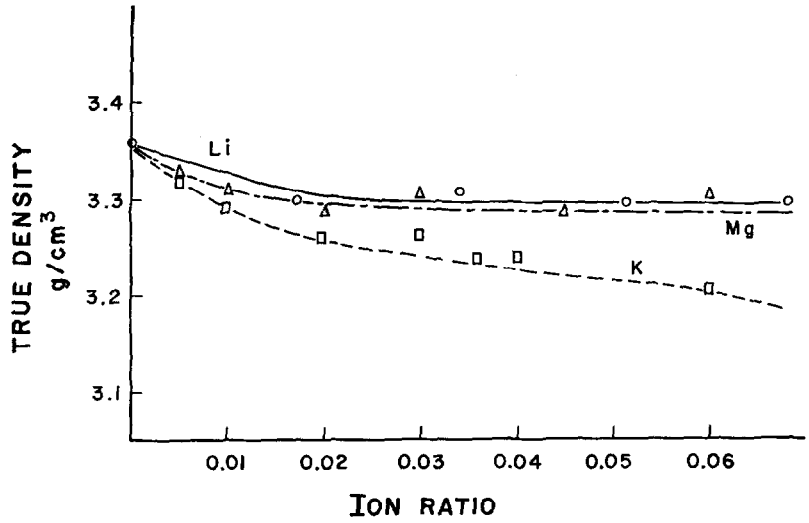

FIG. 2. True densities of impregnated aluminas heated in dry air for 5 hr at 600°C. Probable errors are ±0.04 g/cm³.

heated in the same atmosphere at the same temperature for equal lengths of time, widely divergent physical characteristics appear for samples containing small amounts of various doping agents. The differences in the variation of physical properties with doping and concentration point to effects exclusive from and additive to the characteristic heat- and moisture-induced sintering usually encountered.

Typical values of surface area, micropore volume (pores with diameters less than 700 Å), and true density as a function of concentration and identity of doping agents are presented graphically in Figs. 1 through 3. Measurements of macroscopic properties

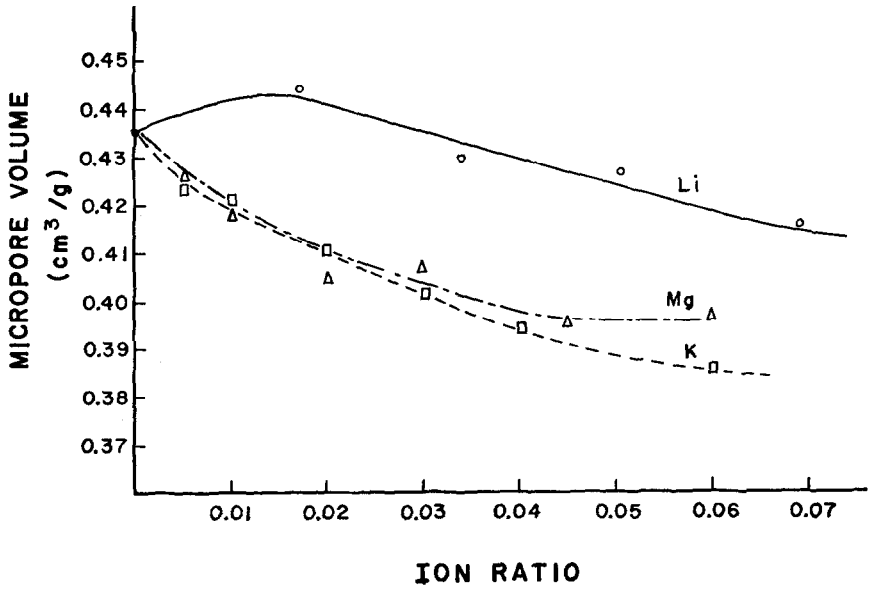

FIG. 3. Cumulative volumes of pores of less than 700-Å diameter in impregnated aluminas heated in dry air for 5 hr at 600°C. Probable errors are ±0.010 cm³/g.

(i.e., macropore volume and particle density) have not been included, as experimental trends are comparable in range with statistical error.

The data shown in Figs. 1 through 3 were taken at a single temperature and atmospheric environment. Variation of these latter parameters invariably led to regular changes in surface area, micropore volume, and density as described previously (*6*, *7*, *8*). We have independently studied surface-area variation with temperature in variously doped aluminas to determine the activation energy for surface loss as a function of impurity concentration. These data are reported below.

X-Ray Diffraction

Some further understanding of the reorganization characterized by the physical measurements may be gained from complementary X-ray diffraction studies. Diffraction patterns were run on all the doped aluminas which had been heated in dry air at 600°C. The Cu $K\alpha$ line generated at a potential of 50 kV and a current of 16 mA and diffracted from the powdered catalyst in a standard G.E. XRD-5 diffraction unit was employed. All the samples gave only three detectable broad maxima, centered at the positions for the [111], [400], and [440] lines of the spinel structure of alumina (*9*). These peaks were always ill-defined, although a substantial gain in crystallinity over the mostly amorphous starting material was observed.

The lithium-doped samples consistently gave the sharpest, most intense lines, while potassium-containing alumina showed the poorest spectra. In the case of lithium, the X-ray data indicated increasing crystallinity with increasing lithium concentration. A strikingly different behavior appeared for the potassium-doped aluminas where apparent crystallinity remained relatively unchanged for potassium contents up to about 0.03 K/Al ion ratio, then decreased at higher

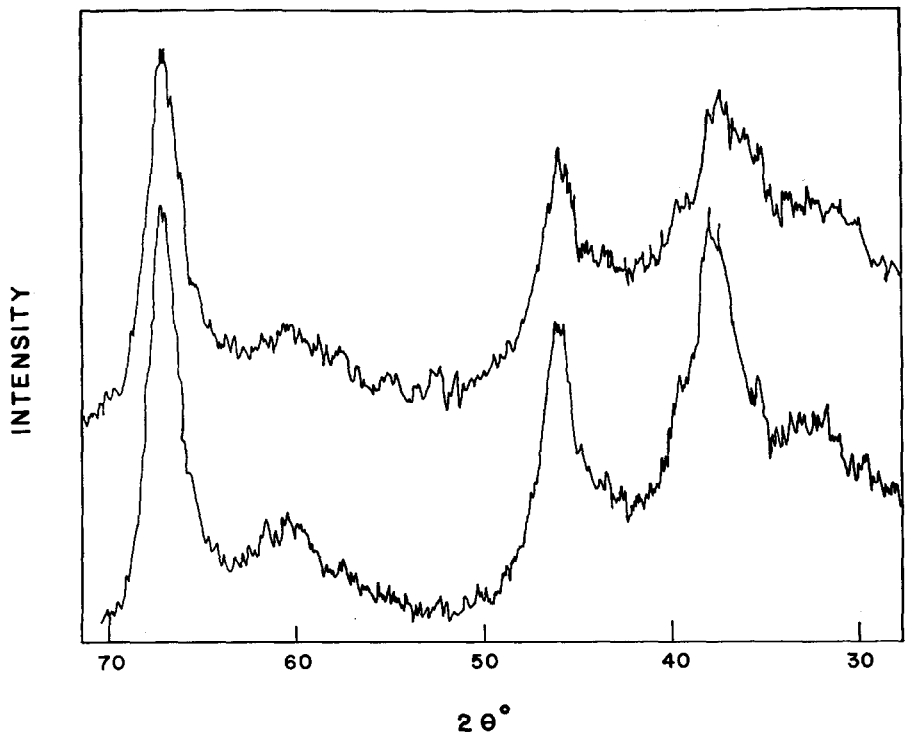

FIG. 4. X-Ray diffraction spectra of spinel-structure aluminas doped with about 0.06 ion ratio K^+ (top) and Li^+ (bottom).

ratios. Magnesium-doped samples showed intermediate properties.

Due to the extremely diffuse character of the diffraction spectra, only qualitative visual comparisons of apparent crystallinity can be made. Typical results, illustrating the type of comparisons referred to in this paper, are shown in Fig. 4, where spectra of lithium- and potassium-doped aluminas of similar foreign-ion content but different crystallinity are shown.

The term "crystallinity" may be extremely misleading, as the source of the line-broadening could be a combination of factors. Either small crystallite sizes or inhomogeneities in lattice constants within a crystallite would broaden the high-angle diffraction lines. Additionally, a high amorphous-material content would raise the background and result in less-pronounced spectral peaks. We feel that the latter source of broadening in our spectra is small, since qualitative observation of the X-ray diffraction spectra in high-angle regions removed from the peaks, and visual survey of electron micrographs indicate only a small purely amorphous phase, in sharp contrast to the unheated starting alumina. This interpretation agrees with conclusions drawn previously from more detailed electron-microscope studies (*10*).

If the line-broadening were a function exclusively of the small crystallite sizes, one could compute the average crystallite size from the Scherrer equation (*11*). From the spectra reported here, crystallite diameters would fall in the range 150–200 Å. Smooth spherical crystallites of this diameter would lead to surface areas of about 60 m^2/g. Irregularly shaped polygons of the same approximate radius could have surface areas an order of magnitude larger. Thus, our experimentally determined surface areas could superficially be attributed to crystallite sizes as derived from X-ray diffraction line-broadening. However, careful observation shows there to be no correlation between surface areas and line width in samples doped with equal concentrations of different ions (see, for example, Figs. 1 and 4). From empirical evidence of this sort, we are forced to conclude that differences in linewidth in the patterns of the differently doped aluminas stem primarily from lattice heterogeneities, and the experimental "apparent crystallinity" may be correlated with the details of the alumina–foreign ion mixed-spinel lattice parameters.

Determination of Reorganization Activation Energy

While any solid with small particle sizes and large surface area is thermodynamically unstable, it has not been determined whether for the aluminas studied here the surface instability derives primarily from energy or entropy considerations. To infer the nature of the driving force in reorganization in these experiments, be it enthalpy or entropy, we have studied the kinetics for the loss of surface area in all of the variously doped aluminas.

The prevalent kinetic treatment (*12*) for diffusion in the solid phase leads to an Arrhenius rate expression for ionic displacement,

$$k = D_0 \exp(-E_D/RT) \qquad (1)$$

where E_D represents the average energy necessary to promote the atoms beyond a potential barrier impeding free migration, and D_0 is proportional to the number of sites capable of experiencing some sort of diffusion. The term D_0 depends upon surface area and pore characteristics, and during sintering will continuously vary, so that the net diffusion in a time t is

$$D = \int_0^t k\,dt = \exp\left(\frac{-E_D}{RT}\right) \int_0^t D_0(t)\,dt. \qquad (2)$$

For a fixed time integral, t, and similar conditions of treatment on the same starting material, we assume as a first approximation that the integral reduces to a constant, k_1. Assuming that the decrease in surface area, S, varies with the amount of diffusion D, through a proportionality constant, k_2, we may express the surface area of the sintered sample by the approximate equation

$$S = S_0 - k_2 k_1 \exp(-E_D/RT), \qquad (3)$$

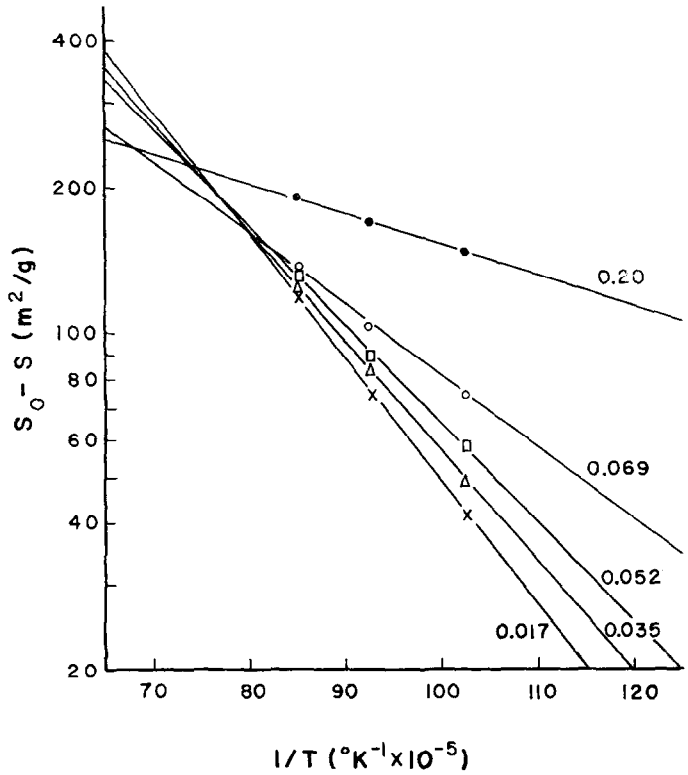

FIG. 5. Arrhenius plots for surface-area loss in lithium-doped aluminas. Ion ratios, Li/Al, are indicated on the appropriate lines.

with S_0 the estimated limiting surface area of the spinel alumina at time zero. A plot of log $(S_0 - S)$ vs. $1/T$ should now yield a straight line with slope proportional to the activation energy of diffusion, E_D. Such a linearity is observed, confirming our assumption of the constancy of k_1. Activation energy plots are shown for the case of several lithium concentrations in Fig. 5.

Typical activation energies for surface loss in these samples are of the order of 3 kcal/mole, a magnitude substantially less than that required for diffusion of cations through the bulk phase or for vapor-phase material transport (*13*). We infer, therefore, that sintering in these samples is predominantly a surface phenomenon, with possible secondary effects induced by bulk- and vapor-phase environments. Moreover, the close parallel between high surface area and high activation energies, exhibited in Table 1, indicates that the surface reorganization is mostly enthalpy-controlled and that any changes or stabilization of surface areas in the experiments described here depend directly upon the surface energy of the unstable alumina and the energy barriers defined in the kinetic description of surface loss.

TABLE 1
ACTIVATION ENERGIES FOR SURFACE REORGANIZATION, AND SURFACE AREAS FOR ALUMINA SAMPLES TREATED AT 600°C[a]

K/Al	S.A. (600°) (m^2/g)	E_c (kcal)	Li/Al	S.A. (600°) (m^2/g)	E_D (kcal)
0.005	176	2.2	0.000	210	4.1
0.01	181	2.4	0.017	235	5.3
0.02	188	2.8	0.035	223	4.6
0.03	198	3.5	0.052	213	4.0
0.04	186	2.8	0.069	197	2.8
0.06	181	2.6	0.20	136	1.4

[a] The potassium-doped samples were heated in the atmosphere, the lithium in a stream of dry air.

Discussion

Although the basic mechanism of sintering in pure spinel alumina seems to be well understood, the effect of the foreign ions adds another dimension to the phenomenon. To account for the nature of the influence of the dopants, we reason that if the samples doped with foreign ions were in complete thermodynamic equilibrium, stable crystalline phases would exist in which the coordination number, symmetry, and interatomic distances were dictated by the well-known basic principles of mineralogy, laid down by Pauling in 1928 (*14*). Although the nature of the impregnation does not lead to complete thermal equilibration, the severity of the temperature treatment and the molecular reorganization incurred must facilitate a partial compromise in the oxygen lattice toward accommodation of the doping agents in stoichiometric configurations tending toward those of a solid-phase thermodynamic equilibrium state. This atomic effect would be most pronounced at or near the surface of those alumina particles exposed to the external environment or within the range defined by the diffusive capacities of the aluminum and the foreign ions. In simpler language, an approximation of stoichiometric phases or compounds exists on or near the surface, the stoichiometry and proportions of such phases dependent upon the identity of the foreign atoms and their concentrations, respectively.

The effect of such a phase on thermal stability was first alluded to by Kordes who claimed an enhanced thermal stability in spinel alumina containing small concentrations of lithium (*15*). In these experiments Kordes determined that the lithium ions occupy octahedrally coordinated cation sites in the spinel lattice, leading to these equilibrium,

$$Al_8[Al_{40/3}\square_{8/3}]O_{32} \xrightleftharpoons{Li_2O} xAl_8[Al_{12}Li_4]O_{32} + Al_2O_3 \quad (4)$$

where the terms in brackets represent octahedrally coordinated cations and the open square denotes an octahedral vacancy found in the pure alumina spinel.

Our data confirm such a stabilization despite the extremely different method of preparation of the doped alumina. At low concentrations of lithium, below about 0.02 Li/Al cation ratio, we find that activation energies for surface loss are quite high (see Fig. 5), and the measured surface areas are larger than in the undoped material. Since one of the primary mechanisms for sintering is diffusion induced by lattice vacancies (*12*), we may rationalize the observed increase in surface area as due to partial removal of this avenue. This is consistent with a surface and bulk more compactly populated, with lattice vacancies effectively filled by available lithium ions.

A semiquantitative calculation of the percentage of the lithium ions, in the 0.0–0.02 ion ratio concentration range, which inhabit the mixed spinel in these experiments, may be made from the decrease in true density and the assumption of a three-phase system containing Al_2O_3, $5Al_2O_3 \cdot Li_2O$, and Li_2O, with densities of 3.36, 3.31, and 2.01 g/cm^3 respectively [the mixed-spinel density computed assuming lattice constants unchanged from pure spinel alumina (*15*)]. Such a calculation leads to the conclusion that at least 70% of the lithium ions in the mixed spinel. If some of the residual lithium ions remaining on the surface reduce the experimentally determined density by blocking the mouths of pores, the percentage occupying the mixed spinel could be even higher.

As lithium concentrations increase beyond about 0.02 ion ratio, occupation by lithium of sites other than existing lattice vacancies apparently begins to occur, and different behaviors of surface area, pore volume, and density appear. X-Ray diffraction data indicate, at this stage, that apparent crystallinity continues to increase, which we attribute to the growth of the mixed-spinel phase. The constancy of true density at concentrations above 0.02 ion ratio also leads to this interpretation, as formation of a mixed spinel from existing pure spinel, blockage of pore mouths, and deposition of Li_2O would all lead to steadily decreasing values. These could only be balanced by the actual crystallization process, the growth of larger crystallites

at the expense of amorphous material, to give a net constancy in density.

The measurements on the magnesium-doped samples lead to a somewhat different interpretation from that for lithium despite the corresponding existence of a mixed spinel having the constitution of the common mineral $Al_2O_3 \cdot MgO$. This spinel has a unit-cell lattice constant of 8.07 Å compared to 7.90 Å for both the pure alumina and the lithium-doped alumina (*15*), so that incorporation of magnesium into the bulk phase by our method of impregnation strains the existing lattice and is energetically less favored than incorporation of lithium. At concentrations above 0.06 ion ratio, some occupation of bulk sites becomes noticeable through a shifting and broadening of the X-ray diffraction spinel lines. Moreover, in this concentration region considerable loss of surface area occurs analogously as a result of the lattice strain caused by the magnesium.

For lower magnesium contents in the range 0.0 to 0.02 ion ratio, surface areas rise from 210 to 218 m^2/g, while specific volume, measured by helium displacement, drops by 0.04 cm^3/g and micropore volume by about the same. Pure deposition of MgO in pores would have about 10% as great an effect upon pore volume and specific volume, so that, initially, some blockage at pore mouths must occur. Between 0.02 and 0.05 ion ratios, pore volume decreases less rapidly, true density levels off, and surface area remains constant. Since formation of the mixed spinel would increase the true density and decrease the surface area, the above behavior implies that large amounts of MgO are remaining on the surface, or in pores, but with decreasing blockage of pore mouths.

The incorporation of potassium into alumina differs in that the existence of a stable potassium-aluminum mixed-spinel lattice has never been reported. The size limitations imposed by the approximate cubic close-packed oxygen ordering of the spinel lattice require ions of smaller ionic radii than that of potassium, so that a local reordering of the oxygen lattice is sterically favored in the vicinity of this cation. Indeed, at temperatures >800°C, a corundum-lattice compound denoted "beta alumina" having the formula $11/Al_2O_3 \cdot K_2O$ has been reported (*16*). This phase is based on an approximate hexagonal close-packing of oxygen atoms, with cations residing in sites of sixfold coordination and symmetry D_{6h}. Although we have been unable to detect a crystalline corundumlike phase in the potassium-doped aluminas, some reorganization of the cation coordination and symmetry in the vicinity of these atoms must necessarily occur.

The data on varying contents of potassium indicate that for concentrations up to about 0.03 K/Al ion ratio, apparent crystallinity as determined by X-ray diffraction remains relatively constant, while surface area rises from 210 to 235 m^2/g. For higher potassium contents, both properties decrease in magnitude. Further departures from the behavior of the lithium-impregnated aluminas are found in the pore volumes which are about 0.03 cm^3/g lower for potassium-doped samples; and in the continual decrease in true density with increasing potassium content.

These data, particularly the low pore volumes, imply that potassium preferentially occupies sites on or near exposed surfaces with little incursion into the bulk spinel lattice. Calculation shows that if all the potassium ions were to reside in pores as K_2O with no blockage of pore mouths, the pore volume would be decreased by about half as much as it is. This fact and the rapidly decreasing density at low potassium contents, accompanied by little change in apparent crystallinity, indicate that even at low concentrations potassium occupation on the surface is quite pronounced and a large amount of pore blockage occurs. Furthermore, surface areas are greater than in the unimpregnated alumina, so that as with magnesium the enhanced cation coordination of surface or near-surface anions near pore openings is manifest in a higher stability with respect to ionic migration. At potassium content above 0.03 ion ratio, the energetically unfavorable squeezing of large potassium ions into small spinel sites in the bulk

begins to outweigh deposition in an energetically favored surface phase, and we observe a decrease in apparent crystallinity due to changes in the lattice constants. Now the increasing lattice strain at phase boundaries encourages sintering, so that we find a concurrent decrease in surface area.

Thus the overall picture for potassium-doped alumina is approximately opposite to that for lithium. Initial potassium impregnate occupies surface sites predominantly near pore openings, with the excess going into the bulk-phase vacancies; while low concentrations of lithium stabilize the existing spinel phase and the overflow creates material of a higher crystallinity.

The duality of the impregnate in these aluminas, the ability to reside either in a stable lattice site or on the surface, may be further demonstrated on a microscopic scale by Mössbauer studies of ferric ions impregnated into alumina. As this duality is critical to our interpretation, these experiments are discussed in some detail below.

Alumina Doped With Fe^{3+}

Iron deposited on alumina may be characterized with respect to valence and symmetry of surroundings through the Mössbauer effect. In these experiments the iron was incorporated in the alumina by exchange with solution of $^{57}Fe(NO_3)_3$ at various pH values. The alumina pellets were then dried at 80°C for 24 hr and, in some cases, calcined in air at 600°C for 6 hr. Spectra were taken on an NSEC Mössbauer spectrometer with a continuous velocity transducer, and recorded on a RIDL 400-channel analyzer. The gamma spectrum was detected by a Reuter-Stokes methane-filled proportional counter operated at 1875 V. A single-channel analyzer selected the 14.4-keV gamma transition for triggering. Mössbauer lines were resolved on a duPont, Model 310, curve fitter.

At the higher pH values (>5) a large amount of iron deposted on the surface, imparting a distinct brownish tinge to the alumina. The Mössbauer spectrum, shown in Fig. 6, is characteristic of α-Fe_2O_3. Kündig *et al.* have shown that the quadruple-split doublet in α-Fe_2O_3 varies with crystallite size, with splittings from 0.42 mm/sec for bulk material to 0.98 mm/sec for the dispersed oxide (*17*). Our average values for 11 determinations fall in about

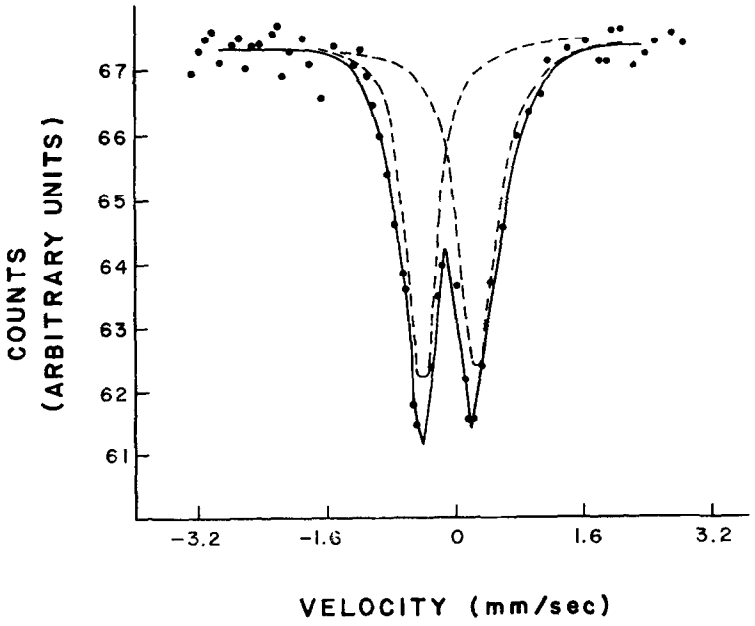

FIG. 6. Mössbauer spectrum of α-Fe_2O_3 deposited as small crystallites on spinel alumina.

the middle of this range, 0.6 ± 0.2 mm/sec.

At lower pH values for deposition, no α-Fe_2O_3 spectrum appears. However, we observe a single very weak line with an isomer shift of about —0.8 mm/sec with respect to iron in stainless steel. We interpret this as arising from ferric ions occupying octahedral sites in the spinel lattice, 300 ppm of iron being present as an impurity in the Al_2O_3.

For low concentrations of impregnate deposited at high pH, or for samples calcined at 600°C, we obtain the doublet comprised of two unequal lines, previously reported by Flinn, Ruby, and Kehl (*18*), and shown in Fig. 7. We propose that this partially represents a superposition of the two spectra described above, with simultaneous detection of α-Fe_2O_3 on the alumina surface, and octahedrally coordinated ferric ions in the bulk phase of the alumina. Several data lend support to this interpretation. The difference in intensity of the two lines increases with severity of calcination, consistent with a diffusion from the surface into the bulk. In addition, the recoil-free fraction becomes surprisingly low, decreasing by a factor of 6 for the high calcination temperature. This may arise from the increased population of ferric ions in unstable defect sites or interstitial positions, or from a Debye temperature lower in the spinel lattice than in α-Fe_2O_3.

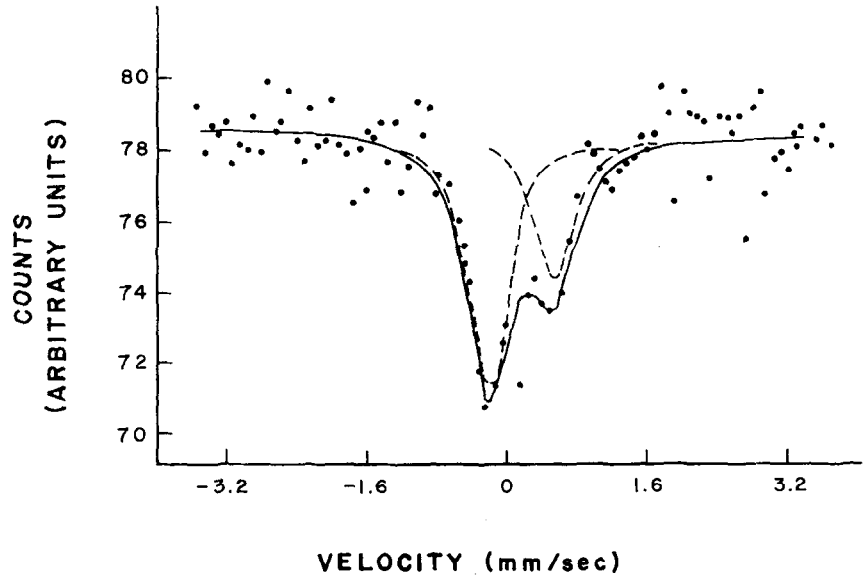

FIG. 7. Mössbauer spectrum of an alumina impregnated with ferric ion and calcined to 600°C.

SUMMARY

The data presented here indicate that it is possible to optimize empirically the stability of transition aluminas through appropriate incorporation of doping agents, to selectively control various physical properties of the alumina, and to offer an explanation for differences in these parameters as a function of the starting material.

The data on varying concentrations of lithium, magnesium, and potassium indicate that thermal stability is a complex parameter sensitive to factors such as inhomogeneities or strains in lattice constants, ionic radii of impregnates, and the relation of the latter to oxygen coordination. Lithium stabilizes a spinel alumina by formation of a mixed bulk phase, while potassium ions give even greater stabilization and reside predominantly in pore mouths. Magnesium ions give an intermediate behavior, with formation of a mixed-spinel phase and surface blocking of pore mouths competing more evenly. The surface sites most involved during impregnation appear to be those near the pore openings. In all

cases, improper concentrations of doping agents result in a loss of surface area in the alumina.

Acknowledgments

We wish to acknowledge the constructive criticism of Dr. James F. Roth and the technical assistance of Mr. Joe Abell and Mr. David Gross.

References

1. Peri, J. B., *J. Chem. Phys.* **69**, 211 (1965).
2. Newsome, J. D., Heiser, H. W., Russell, A. S., and Stumpf, H. C., "Alumina Properties." Aluminum Company of America, Pittsburgh, Pennsylvania, 1960.
3. Pines, H., and Haag, W. O., *J. Am. Chem. Soc.* **82**, 2471 (1960).
4. Smith, A. E., and Beeck, O. A., U. S. Patent No. 2,454,227 (Nov. 16, 1948); U. S. Patent No. 2474,440 (June 28, 1949).
5. Brunauer, H., Emmett, P. H., and Teller, E., *J. Am. Chem. Soc.* **60**, 309 (1938).
6. Schlaffer, W. G., Adams, C. R., and Wilson, J. N., *J. Phys. Chem.* **69**, 1530 (1965).
7. Schlaffer, W. G., Morgan, C. Z., and Wilson, J. N., *J. Phys. Chem.* **61**, 714 (1957).
8. Adams, C. R., and Voge, H. H., *J. Phys. Chem.* **61**, 722 (1957).
9. Ervin, G., *Acta Cryst.* **5**, 103 (1952).
10. Ginsberg, H., Huttig, W., and Strunk-Lichtenberg, G., *Z. Anorg. Allgem. Chem.* **293**, 33 (1957).
11. Schossberger, F., *in* "Encyclopedia of X-rays and Gamma Rays" (G. L. Clark, ed.), pp. 728–732. Reinhold, New York, 1963.
12. Gray, T. J., *in* "The Defect Solid State" (T. J. Gray, ed.), pp. 77–138. Interscience, New York, 1957.
13. Toropov, N. A., and Barzakovskii, V. P., *in* "High Temperature Chemistry of Silicates and Other Oxide Systems." Consultants Bureau, New York, N. Y., 1966.
14. Pauling, L., "The Nature of the Chemical Bond," 3rd ed., pp. 505–562. Cornell Univ. Press, Ithaca, New York, 1960.
15. Kordes, E., *Z. Krist.* **91**, 193 (1935).
16. Levin, E. M., Robbins, C. R., and McMurdie, H. F., *in* "Phase Diagrams for Ceramists" (M. K. Reser, ed.), p. 651. The American Ceramic Society, Columbus, Ohio, 1964.
17. Kündig, W., Bommel, H., Constabaris, G., and Lindquist, R. H., *Phys. Rev.* **142**, 327 (1966).
18. Flinn, P. A., Ruby, S. L., and Kehl, W. L., *Science* **143**, 1434 (1964).